

Implications of $\bar{\nu}_e e^- \rightarrow W^- \gamma$ for high-energy $\bar{\nu}_e$ observation

H. Athar^{1,2,*} and Guey-Lin Lin^{2,†}

¹*Physics Division, National Center for Theoretical Sciences, Hsinchu 300, Taiwan*

²*Institute of Physics, National Chiao Tung University, Hsinchu 300, Taiwan*

(November 4, 2018)

Absorption of high-energy $\bar{\nu}_e$ over electrons above the W boson production threshold is reexamined. It is pointed out that, in the case of photon emissions along the direction of incident high-energy $\bar{\nu}_e$, the kinematically allowed average energy carried by the final state hard photon can be $\leq 1\%$ of the incident $\bar{\nu}_e$ energy above the W boson production threshold. The differential energy spectrum for the final state hard photon is calculated. We also discuss implications of our results for the prospective search of high-energy $\bar{\nu}_e$ through this final state hard photon.

PACS number(s): 12.15.Ji, 13.15.+g, 14.70.Bh, 98.70.Sa

A positive observation of high-energy neutrinos above the atmospheric background will mark the beginning of high-energy neutrino astronomy. Several high-energy neutrino detectors, commonly known as high-energy neutrino telescopes, are currently at a rather advanced stage of their deployments. This necessitates the identification of possible signatures of the high-energy neutrino interactions, particularly those occurring inside the high-energy neutrino telescopes. Needless to mention, such studies will complement the high-energy gamma ray astronomy for understanding the origin of high-energy radiation from the cosmos [1].

In this *Brief Report*, we reexamine in some detail the energy spectrum of the final-state hard photon in the absorption process $\bar{\nu}_e e^- \rightarrow W^- \gamma$ above the W -boson production threshold. This absorption process has been discussed in Ref. [2], whereas its closely associated resonant absorption process $\bar{\nu}_e e^- \rightarrow W^- (\rightarrow \bar{\nu}_\mu \mu^-)$, now referred to as ‘‘Glashow resonance’’, occurring at $E_{\bar{\nu}_e}^{res} = M_W^2 / (2m_e) \sim 6.3 \cdot 10^6$ GeV, was first pointed out in Ref. [3], and was subsequently studied in Ref. [4]. However, to our knowledge, the energy spectrum of the final-state photon in $\bar{\nu}_e e^- \rightarrow W^- \gamma$ has not been studied before. Here, we shall give an estimate of the kinematically allowed average energy for the hard photon and calculate the photon energy spectrum as well as the total cross section of the absorption process $\bar{\nu}_e e^- \rightarrow W^- \gamma$.

There are two Feynman diagrams contributing to the absorption process, $\bar{\nu}_e e^- \rightarrow W^- \gamma$

*E-mail: athar@phys.cts.nthu.edu.tw

†E-mail: glin@cc.nctu.edu.tw

in the leading order. They are shown in Fig. 1. Out of these two diagrams, diagram (b) contains a W -boson exchange, hence its contribution is suppressed for the range of \sqrt{s} under discussion (see later).

The energy of the outgoing photon in the center-of-mass (CM) frame is given by

$$E_\gamma^{CM} = \frac{s - M_W^2}{2\sqrt{s}}, \quad (1)$$

where $s = 2m_e E_{\bar{\nu}_e}$. The range of \sqrt{s} of interest to us is $\sqrt{s_0} < \sqrt{s} < \frac{6}{5}\sqrt{s_0}$, where $\sqrt{s_0} \equiv M_W + \Gamma_W$. The lower limit for \sqrt{s} is chosen to distinguish our signature from that due to the soft photon emission in the resonant absorption process $\bar{\nu}_e e^- \rightarrow W^-$. The upper limit of \sqrt{s} is the largest incident energy such that $\bar{\nu}_e e^- \rightarrow W^- \gamma$ remains dominant over other competing processes (see discussions below). Substituting $\sqrt{s} = \sqrt{s_0}$ in Eq. (1), we obtain

$$E_\gamma^{CM} \simeq \Gamma_W. \quad (2)$$

We then apply the Lorentz boost to obtain the photon energy in the Lab frame, or in a high-energy neutrino telescope. For a photon moving precisely collinear to the incident neutrino, its energy in the Lab frame is given by

$$E_\gamma \simeq \Gamma_W \sqrt{\frac{2E_{\bar{\nu}_e}}{m_e}} \simeq \frac{M_W \Gamma_W}{m_e}. \quad (3)$$

Note that the boost factor $\sqrt{2E_{\bar{\nu}_e}/m_e}$ significantly enhances the photon energy with respect to its CM value. According to Eq. (3), E_γ is roughly 5% of $E_{\bar{\nu}_e}$. We emphasize that this is the maximal energy that the outgoing photon can carry. Let us also remark that, for the absorption process $\bar{\nu}_e e^- \rightarrow W^- \gamma$, the movement of target electrons inside atoms (in water) does not lead to any appreciable change in the emitted photon energy.

To calculate the differential photon spectrum, it is convenient to define the dimensionless variables, $\lambda = s/M_W^2$, and $y = E_\gamma/E_{\bar{\nu}_e}$. In terms of λ and y , the differential photon energy spectrum reads:

$$\frac{d\sigma}{dy} = \frac{\sqrt{2}\alpha G_F}{\lambda^2(\lambda - 1)^2} [(\lambda - 1)(\lambda^2 + 1)y^{-1} + 4\lambda^2(\lambda - 1)y - 2\lambda^3 y^2 - \lambda(3\lambda^2 - 4\lambda + 3)]. \quad (4)$$

The above equation implies that the final-state photon is more likely to carry a smaller energy fraction from the incoming high-energy neutrino, namely it prefers to move back-to-back to the neutrino. The minimal and maximal values for y are given by $y_{min} = m_e^2/s$ and $y_{max} = (\lambda - 1)/\lambda$ respectively. For $\sqrt{s} = \sqrt{s_0}$, i.e., $\lambda = 1 + \Gamma_W/M_W$, we obtain the value of maximal photon energy as stated in Eq. (3). Clearly y_{max} increases with the CM energy $\sqrt{s} \equiv M_W \sqrt{\lambda}$. However, as \sqrt{s} increases, the differential cross section $d\sigma/dy$ decreases. The behaviors of $d\sigma/dy$ for a few representative values of λ are depicted in Fig. 2. From the

behaviors of $d\sigma/dy$, one can compute the average y value, which is of more observational interest, as a function of the incoming energy λ :

$$\langle y \rangle = \frac{\int y \frac{d\sigma}{dy} dy}{\int \frac{d\sigma}{dy} dy}. \quad (5)$$

The quantity $\langle y \rangle$ is basically the average fraction of the incident $E_{\bar{\nu}_e}$ that is carried by the hard photons in the Lab frame. The denominator on the R.H.S. of the above equation is just the total cross section which can be calculated by integrating Eq. (4) over y . This gives

$$\sigma_{\bar{\nu}_e e^- \rightarrow W^- \gamma} = \frac{\sqrt{2}\alpha G_F}{3\lambda^2(\lambda-1)} \left[3(\lambda^2+1) \ln \left(\frac{M_W^2(\lambda-1)}{m_e^2} \right) - (5\lambda^2 - 4\lambda + 5) \right]. \quad (6)$$

The cross section $\sigma_{\bar{\nu}_e e^- \rightarrow W^- \gamma}$ given by Eq. (6) depends only on the CM energy λ . Numerically, the logarithmic factor in the above equation dominates for $\lambda \simeq 1$ as well as for $\lambda \gg 1$. Our result for $\sigma_{\bar{\nu}_e e^- \rightarrow W^- \gamma}$ agrees with the one given by Brown *et al.* in Ref. [2]. However, it disagrees with the result by Seckel in the same reference. The numerator on the R.H.S. of Eq. (5) can be calculated in a similar way. In this case, one may set $y_{min} = 0$. We find

$$\int y \frac{d\sigma}{dy} dy = \frac{\sqrt{2}\alpha G_F}{3\lambda^3} (\lambda^2 + \lambda + 1). \quad (7)$$

The values of $\langle y \rangle$ for the energy range of interest to us are as follows: $\langle y \rangle \simeq 1.3 \cdot 10^{-3}$ for $E_{\bar{\nu}_e} = 6.6 \cdot 10^6$ GeV, $\langle y \rangle \simeq 6.0 \cdot 10^{-3}$ for $E_{\bar{\nu}_e} = 8.6 \cdot 10^6$ GeV, whereas $\langle y \rangle \simeq 9.7 \cdot 10^{-2}$ for $E_{\bar{\nu}_e} = 1.1 \cdot 10^7$ GeV.

It is important to compare the cross section of $\bar{\nu}_e e^- \rightarrow W^- \gamma$ with the cross sections of conventional channels. The behaviors of these cross sections as functions of $E_{\bar{\nu}_e}$ are shown in Fig. 3. In this figure, we have included, besides the cross section of the current process, the resonant cross section, $\sigma_{\bar{\nu}_e e^- \rightarrow W^- \rightarrow \text{hadrons}}$, taken¹ from Ref. [5], as well as the charged current deep-inelastic $\bar{\nu}_e$ scattering cross section over nuclei, $\sigma_{\bar{\nu}_e N \rightarrow e^+ X}^{CC}$, taken from Ref. [7] with CTEQ4-DIS parton distributions. We should remark that the other modern sets of parton distribution functions only make small differences in the value of $\sigma_{\bar{\nu}_e N \rightarrow e^+ X}^{CC}$. From Fig. 3, we note that $\sigma_{\bar{\nu}_e e^- \rightarrow W^- \gamma}$ dominates over the other two for less than half an order of magnitude in $E_{\bar{\nu}_e}$ ($7 \cdot 10^6 \leq E_{\bar{\nu}_e}/\text{GeV} \leq 1 \cdot 10^7$). The dominance is however within a factor of 2. The effect of this absorption process can be viewed as an extended (high-energy) tail of the resonant absorption process $\bar{\nu}_e e^- \rightarrow W^-$ above the W -boson production threshold. This enhancement is due to the t -channel exchange of a nearly on-shell electron [see Fig. 1(a)].

¹This cross section differs from that used in Ref. [6] by a factor of 2. This discrepancy might be due to an incorrect spin averaging assumed in Ref. [6].

Note that, for the relevant $E_{\bar{\nu}_e}$ range, the absorption process $\bar{\nu}_e e^- \rightarrow W^- \gamma$ is the unique process with a direct emission of hard photons and a comparable cross section with the deep-inelastic $\bar{\nu}_e$ scattering cross section over nuclei. Concerning the search for high-energy $\bar{\nu}_e$, the absorption process over electrons has the advantage that $\sigma_{\bar{\nu}_e e^-}$ is basically free from any theoretical uncertainties unlike $\sigma_{\bar{\nu}_e N}$.

A relevant remark is in order. In Ref. [8], assuming an intrinsic relative ratio among high-energy electron, muon and tau neutrinos as 1: 2: 0 in units of intrinsic electron neutrino flux, and using the then available constraints on neutrino mixing parameters (namely δm^2 and $\sin^2 2\theta$), it was shown that for cosmologically distant sources of high-energy neutrinos, this relative ratio becomes 1: 1: 1 again in units of intrinsic electron neutrino flux, due to neutrino flavor oscillations during the propagation of high-energy neutrinos. Here electron neutrino stands for the sum of electron and anti electron neutrino and like wise. In the relevant $E_{\bar{\nu}_e}$ range, the change in the relative ratio of the intrinsic high-energy neutrino fluxes due to neutrino flavor oscillations essentially neither depends on $E_{\bar{\nu}_e}$, nor on the value of neutrino mixing parameters, as the three relative ratios differ by no more than $\sim 10\%$ from 1: 1: 1 (and is due to the present range of uncertainties in neutrino mixing parameters). This implies that, in the relevant $E_{\bar{\nu}_e}$ range, the (downward going) intrinsic high-energy electron neutrino flux is least affected by neutrino flavor oscillations, both in its intrinsic energy dependence as well as in its absolute value. The high-energy muon neutrino flux changes by $\sim 50\%$, whereas the high-energy tau neutrino flux changes even more with respect to its intrinsic value. Therefore, it follows that, for a $E_{\bar{\nu}_e}$ range that $\sigma_{\bar{\nu}_e e^- \rightarrow W^- \gamma}$ dominates over other competing cross sections, a prospective search for hard photons in $\bar{\nu}_e e^- \rightarrow W^- \gamma$ may constrain/measure the *intrinsic* $\bar{\nu}_e$ flux with minimal neutrino flavor oscillation effect. In the case where the constraints for ν_e intrinsic flux exist for the aforementioned energy range, one can even obtain information on the neutrino oscillation scenarios that lead to a change in the $\bar{\nu}_e$ to ν_e ratio with respect to its intrinsic value (for instance, ~ 1) [9].

We have estimated the downward going event rate for the absorption process $\bar{\nu}_e e^- \rightarrow W^- \gamma$ by using the following equation:

$$\text{Rate} = \frac{10}{18} A \int dE_{\bar{\nu}_e} P_\gamma(E_{\bar{\nu}_e}) \frac{dN}{dE_{\bar{\nu}_e}}, \quad (8)$$

where A is the area of the high-energy neutrino telescope in ice (or water), which we take as 1 km², the integration over $E_{\bar{\nu}_e}$ is performed over the energy range that $\bar{\nu}_e e^- \rightarrow W^- \gamma$ dominates, and $P_\gamma(E_{\bar{\nu}_e})$ is given by

$$P_\gamma(E_{\bar{\nu}_e}) = N_A \int dy R_\gamma(y, E_{\bar{\nu}_e}) \frac{d\sigma}{dy}, \quad (9)$$

where $N_A = 6 \cdot 10^{23} \text{ cm}^{-3}$ (water equivalent) is the Avogadro's number, $d\sigma/dy$ is given by Eq. (4), while the limits for y are indicated right after that equation. For simplicity, we take

$R_\gamma(y, E_{\bar{\nu}_e}) \simeq R_e(y, E_{\bar{\nu}_e})$ as an approximation, where the latter is the electron range given by [10,11]

$$R_e(y, E_{\bar{\nu}_e}) \simeq 40 \text{ cmwe} \left[(1 - \langle y(E_{\bar{\nu}_e}) \rangle) \left(\frac{E_{\bar{\nu}_e}}{6.2 \cdot 10^4 \text{ GeV}} \right) \right]^{\frac{1}{2}}. \quad (10)$$

In Eq. (8), the $dN/dE_{\bar{\nu}_e}$ is the downward going differential $\bar{\nu}_e$ flux arriving at the high-energy neutrino telescope. For $dN/dE_{\bar{\nu}_e}$, we consider the gamma ray burst fireball model proposed in Ref. [12] as an example, where $p\gamma$ interactions are suggested to produce the high-energy $\bar{\nu}_e$ flux at the gamma ray burst fireball, such that

$$\frac{dN}{dE_{\bar{\nu}_e}} \simeq \frac{1}{2} \cdot \frac{1}{2} \cdot 4 \cdot 10^{-8} \left(\frac{E_{\bar{\nu}_e}}{1 \text{ GeV}} \right)^{-2} \text{ cm}^{-2} \text{ s}^{-1} \text{ sr}^{-1} \text{ GeV}^{-1}, \quad (11)$$

for the relevant $E_{\bar{\nu}_e}$ range. Here we have ignored the effect of neutrino flavor oscillations in light of earlier discussions. In Eq. (11), the first factor of $\frac{1}{2}$ arises because half of the electron neutrino flux is considered to be of anti electron neutrino type and the second factor of $\frac{1}{2}$ arises because the electron neutrino flux is considered to be one half of the muon neutrino flux.

The event rate turns out to be $\sim 3 \cdot 10^{-4}$ in units of per year per steradian with 1 km² area and is therefore less than the event rates of other $\bar{\nu}_e$ interaction channels in the same $E_{\bar{\nu}_e}$ range [7]. The event rate for the prospective observation of direct hard photon in the typical high-energy neutrino telescope is rather low because of the small R_γ value, the rather limited range for $E_{\bar{\nu}_e}$, and the high-energy $\bar{\nu}_e$ flux model being considered. If we take the present upper bound for the diffuse high-energy neutrino flux set by AMANDA B10 [13] as the value for high-energy $\bar{\nu}_e$ flux, then the event rate is correspondingly higher up to approximately two orders of magnitude.

Given the current capabilities of typical high-energy neutrino telescopes, the shower generated by the hard photon is not easy to be separated from the one generated by the W -boson inside the high-energy neutrino telescope, mainly because of a rather small R_γ value. The signature of this absorption process in terms of event topology is thus similar to that of other $\bar{\nu}_e$ interaction channels for the relevant $E_{\bar{\nu}_e}$ range in the high-energy neutrino telescopes.

In the context of prospective search for high-energy $\bar{\nu}_e$, there can be few other circumstances where the hard photon emission in the absorption process $\bar{\nu}_e e^- \rightarrow W^- \gamma$ is of some interest. For instance, if a high-energy $\bar{\nu}_e$ crosses a region of relatively intense e^- concentration, the hard photon with $E_\gamma \sim O(10^4)$ GeV will be emitted along with the W -boson (note, in this context, the absorption process, $\nu_e e^+ \rightarrow W^+ \gamma$, also leads to a hard photon emission along the direction of incident high-energy ν_e for the same \sqrt{s} range). If the scattering length of this hard photon is less than (or comparable to) the distance between this region and the prospective detector, one expects that some part of the (electromagnetic) shower generated by this hard photon may be measured. If such a measurement can

be implemented, one should be able to constrain the flux of high-energy $\bar{\nu}_e$. This type of experiment is complementary to the prospective direct observation of high-energy $\bar{\nu}_e$ flux through the high-energy neutrino telescopes. An example can be that the absorption process $\bar{\nu}_e e^- \rightarrow W^- \gamma$ takes place along the surface of the earth and the emitted hard photon generates an air shower (as well as the W -boson generated shower) that propagates upward (or in the nearly horizontal direction) in the atmosphere of the earth. The future downward facing space (or possibly balloon) based shower detectors, if deployed relatively nearby, may eventually become sensitive to these showers [14]. The secondaries in the nearly horizontal showers generated by hard photons with $E_\gamma \sim O(10^4)$ GeV can, in principle, be searched in the appropriate ground based detectors as well [15].

ACKNOWLEDGMENTS

H.A. thanks Physics Division of NCTS for financial support. G.L.L. is supported by the National Science Council of R.O.C. under the grant number NSC89-2112-M009-041. This work is carried out under the auspices of the NCTS topical program *Fields and Structures in the Expanding Universe*.

-
- [1] For recent review articles, see, for instance, J. G. Learned and K. Mannheim, *Ann. Rev. Nucl. Part. Sci.* **50**, 679 (2000); F. Halzen, *Phys. Rept.* **333**, 349 (2000), and references cited therein.
- [2] R. W. Brown, D. Sahdev and K. O. Mikaelian, *Phys. Rev. D* **20**, 1164 (1979); K. O. Mikaelian and I. M. Zheleznykh, *Phys. Rev. D* **22**, 2122 (1980); V. S. Berezinskiĭ and A. Z. Gazizov, *Sov. J. Nucl. Phys.* **33**, 120 (1981) [*Yad. Fiz.* **33**, 230 (1981)]; F. Wilczek, *Phys. Rev. Lett.* **55**, 1252 (1985); D. Seckel, *Phys. Rev. Lett.* **80**, 900 (1998) [hep-ph/9709290].
- [3] S. L. Glashow, *Phys. Rev.* **118**, 316 (1960).
- [4] J. N. Bahcall and S. C. Frautschi, *Phys. Rev.* **135B**, 788 (1960); V. S. Berezinskiĭ and A. Z. Gazizov, *JETP Lett.* **25**, 254 (1977) [*Pisma Zh. Eksp. Teor. Fiz.* **25**, 276 (1977)]; V. S. Berezinsky, D. Cline and D. N. Schramm, *Phys. Lett. B* **78**, 635 (1978); I. M. Zheleznykh and É. A. Tainov, *Sov. J. Nucl. Phys.* **32**, 242 (1980) [*Yad. Fiz.* **32**, 468 (1980)]; V. S. Berezinsky and V. L. Ginzburg, *Mon. Not. R. Astr. Soc.* **194**, 3 (1981); R. W. Brown and F. W. Stecker, *Phys. Rev. D* **26**, 373 (1982); G. Domokos and S. Kovesi-Domokos, *Phys. Lett. B* **346**, 317 (1995) [hep-ph/9410352].
- [5] T. K. Gaisser, F. Halzen and T. Stanev, *Phys. Rept.* **258**, 173 (1995) [Erratum-ibid. **271**, 355 (1996)] [hep-ph/9410384].

- [6] P. B. Price, *Astropart. Phys.* **5**, 43 (1996) [astro-ph/9510119].
- [7] R. Gandhi, C. Quigg, M. H. Reno and I. Sarcevic, *Phys. Rev. D* **58**, 093009 (1998) [hep-ph/9807264].
- [8] H. Athar, M. Jeżabek and O. Yasuda, *Phys. Rev. D* **62**, 103007 (2000) [hep-ph/0005104], and references cited therein.
- [9] See, for instance, M. A. Mughal and H. Athar, hep-ph/9806408.
- [10] R. Gandhi, C. Quigg, M. H. Reno and I. Sarcevic, *Astropart. Phys.* **5**, 81 (1996) [hep-ph/9512364].
- [11] T. Stanev, C. Vankov, R. E. Streitmatter, R. W. Ellsworth and T. Bowen, *Phys. Rev. D* **25**, 1291 (1982).
- [12] E. Waxman and J. Bahcall, *Phys. Rev. Lett.* **78**, 2292 (1997) [astro-ph/9701231].
- [13] See, for instance, M. Kowalski, talk given at *International Euorphysics Conference on High Energy Physics* (EPS HEP 2001), Budapest (Hungary), 2001 (to appear in its proceedings).
- [14] G. Domokos and S. Kovesi-Domokos, hep-ph/9805221; D. Fargion, astro-ph/0002453. For a recent review article, see, D. B. Cline and F. W. Stecker, astro-ph/0003459.
- [15] See, for instance, R. A. Ong, *Phys. Rept.* **305**, 93 (1998).

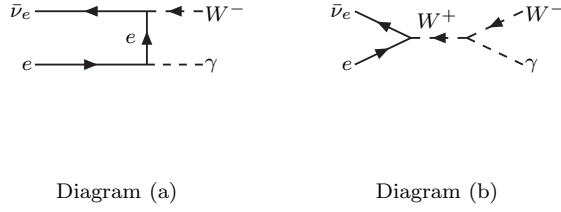


FIG. 1. The Feynman diagrams contributing to $\bar{\nu}_e e^- \rightarrow W^- \gamma$ in the leading order.

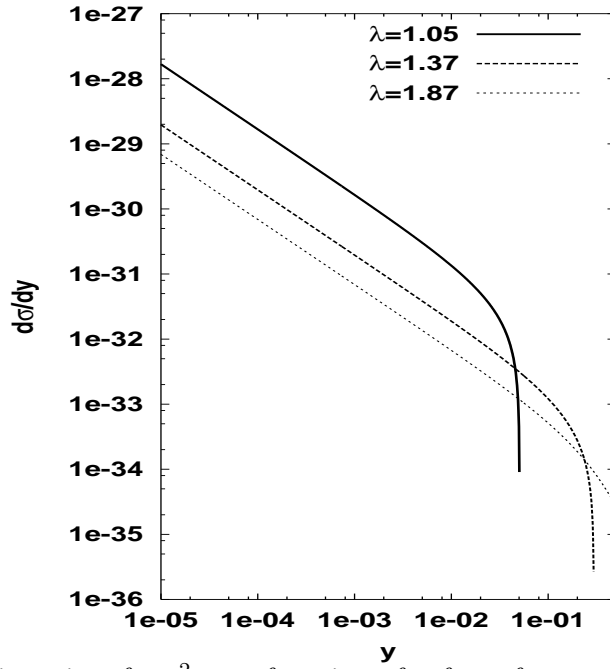


FIG. 2. The $d\sigma/dy$ in units of cm^2 as a function of y for a few representative values of λ [see Eq. (4)]. $\lambda = 1.05$ corresponds to $E_{\bar{\nu}_e} = 6.6 \cdot 10^6$ GeV, $\lambda = 1.37$ corresponds to $E_{\bar{\nu}_e} = 8.6 \cdot 10^6$ GeV, whereas $\lambda = 1.87$ corresponds to $E_{\bar{\nu}_e} = 1.1 \cdot 10^7$ GeV.

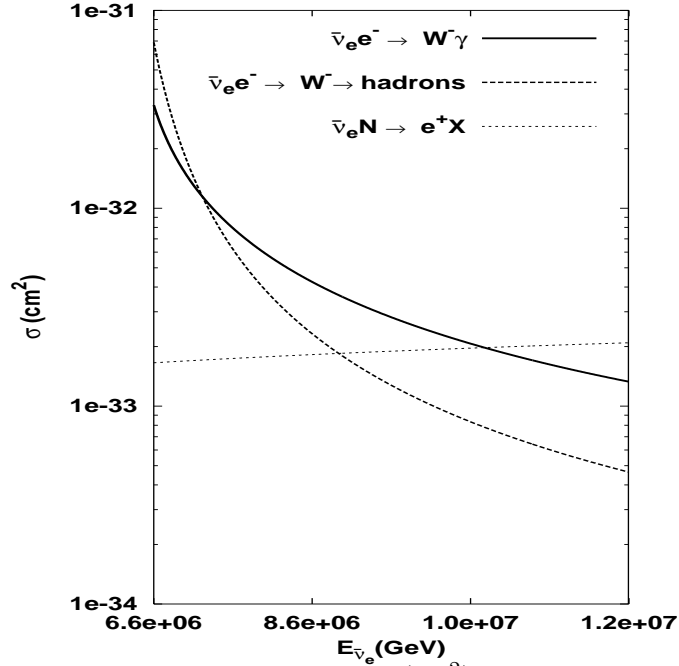


FIG. 3. High-energy $\bar{\nu}_e$ absorption cross section σ (cm^2), over two different target particles as a function of electron anti neutrino energy $E_{\bar{\nu}_e}$ (GeV). The minimum value of $E_{\bar{\nu}_e}$ corresponds to $(M_W + \Gamma_W)^2/2m_e$. Solid curve is obtained using Eq. (6). Dashed and dotted curves are from Ref. [5] and Ref. [7], respectively.